Computational Methods for Differential Equations
http://cmde.tabrizu.ac.ir
Vol. 8, No. 4, 2020, pp. 685-707
DOI:10.22034/cmde.2020.27817.1374

The use of CESTAC method to find optimal shape parameter and optimal number of points in RBF-meshless methods to solve differential equations

Hasan Barzegar Kelishami
Department of Mathematics, Central Tehran Branch,
Islamic Azad University, Tehran, Iran.
E-mail: hb.math@yahoo.com

Mohammad Ali Fariborzi Araghi*
Department of Mathematics, Central Tehran Branch,
Islamic Azad University, Tehran, Iran.
E-mail: m_fariborzi@iauctb.ac.ir, fariborzi.araghi@gmail.com

Majid Amirfakhrian
Department of Mathematics, Central Tehran Branch,
Islamic Azad University, Tehran, Iran.
E-mail: amirfakhrian@iauctb.ac.ir

Abstract One of the schemes to find the optimal shape parameter and optimal number of points in the radial basis function (RBF) methods is to apply the stochastic arithmetic (SA) in place of the common floating-point arithmetic (FPA). The main purpose of this work is to introduce a reliable approach based on this new arithmetic to compute the local optimal shape parameter and number of points in multiquadric and Gaussian RBF-meshless methods for solving differential equations, in the iterative process. To this end, the CESTAC method is applied. Also, in order to implement the proposed algorithms, the CADNA library is performed. The examples illustrate the efficiency and importance of using this library to validate the results.

Keywords. Stochastic Arithmetic, CESTAC method, CADNA library, Differential equation, Radial basis function (RBF).

2010 Mathematics Subject Classification. 34B05, 34L30, 35A09, 65MXX, 65L10.

1. Introduction

Consider a general class of boundary or initial value problems under a domain Ω with boundary $\partial\Omega$, and linear differential operators $\mathcal{L}$ and $\mathcal{B}$:

$$\mathcal{L}u = f,\ x \in \Omega \subset \mathbb{R}^d;\ \mathcal{B}u|_{\partial\Omega} = g. \tag{1.1}$$

In recent years, some authors worked on finding the optimal shape parameter and optimal number of points, in solving differential equations based on RBF like Bayona et al. in [8, 10, 11], Afiatdoust, Esmaeilbeigi in [5] and Uddin in [39]. Also, Sarra and Sturgill [30] presented a random variable shape parameter ϵ strategy and

Received: 9 June 2018 ; Accepted: 16 June 2019.
* Corresponding author.

applied it for interpolation and two-dimensional linear elliptic boundary value problems. Kansa [25, 26] presented an exponential variable shape parameter ϵ strategy that uses a different value of the shape parameter at each center. Moreover, Luh [28, 29] worked on finding optimal shape parameter in the interpolation functions. In [26, 37], exponential variable shape parameters ϵ_j are considered as below:

$$\epsilon_j = \left(\epsilon_{\min}^2 \left(\frac{\epsilon_{\max}^2}{\epsilon_{\min}^2} \right)^{(j-1)/(N-1)} \right)^{1/2}, j = 1, 2, ..., N.$$

In [32, 37], the random variable shape parameters ϵ_j are recommended as follows:

$$\epsilon_j = \epsilon_{\min} + (\epsilon_{\max} - \epsilon_{\min}) \times rand(1, N),$$

the rand is the MATLAB functions that return uniformly distributed pseudo-random numbers on the unit interval. In [37], the trigonometric variable shape parameters ϵ_j strategy is proposed as

$$\epsilon_j = \epsilon_{\min} + (\epsilon_{\max} - \epsilon_{\min}) \times \sin(j), \ j = 1, 2, ..., N.$$

In these three strategies mentioned exponential, random and trigonometric, according to what has been indicated in Ref. [37], $\epsilon_{\min} = 1/\sqrt{N}$ and $\epsilon_{\max} = 3/\sqrt{N}$ have been considered.

In this paper, we deal with finding reasonable variable shape parameters by taking a different approach. The purpose is to use a search algorithm using SA (stochastic arithmetic) to determine optimal variable shape parameters ϵ_j.

In the FPA (floating-point arithmetic), usually the proposed algorithms of RBF are implemented by a package like Matlab, Mathematica or Maple and in most cases a fixed value is considered for shape parameter or number of points. Also, the termination criterion depends on a positive number like *eps* as the accuracy. The FPA is not able to rely on the results and detect any instabilities during the run of the program. So, the final results may not be accurate or the number of iterations may increase without increasing the accuracy of the results. In this case, because of the round-off error propagation, the computer may not be able to improve the accuracy of the computed solution. Therefore, the validation of the computed results is important.

In Eq. (1.1), the meshless points $\{x_k\}_{k=1}^N \subset \Omega$ and in two-dimensional $\{(x_k, y_k)\}_{k=1}^N$ is selected based on Gaussian (GA) as $\psi(r) = e^{-\epsilon^2 r^2}$ or multiquadrics (MQ) as $\psi(r) = \sqrt{\epsilon^2 + r^2}$ RBF method, where r is the distance between the grid points. These functions depend on ϵ, known as the shape parameter, that has an important role in approximation theory using RBFs.

This study provides new insights into RBF-meshless method. The main issues are:
a) To obtain the optimal computed solution of differential equations in a reliable scheme,
b) To determine the optimal shape parameter ϵ by changing the number of nodal points N,
c) To determine the optimal number of nodal points N by changing the shape parameter ϵ.

In order to gain access to these goals and validate the numerical results, as well as, control round-off errors, we use the CESTAC[1] method [41, 42] and CADNA[2] library [16] according to the rules of the SA. In [1, 13, 18, 20, 27], the researchers worked on the SA, the CESTAC method and the CADNA library.

In this essay, we present a strategy to control the shape parameter in the RBF for solving the differential equations, also we determine the optimal number of points, and find the suitable approximate solution of the differential equation at the nodal points so that the local truncation errors are minimized. It is shown that the CESTAC method and the CADNA library[16, 23] are efficient tools to validate the results and get the optimal values. The essay has been organised in the following way. In section 2, a brief description of the CESTAC method is reminded. In section 3, we explain the main idea which offers a reliable scheme based on the SA in discrete case and the CESTAC method to solve a differential equation via the RBF-meshless method. In this case, some algorithms are presented to implement by means of the CADNA library. In section 4, some numerical examples are solved to illustrate the importance of using the SA to validate the results of the proposed algorithms.

2. Preliminaries

In this section, the CESTAC method is reminded. The main tasks of the CESTAC method are defined in[34, 40, 41, 42, 43, 44] which are:

- simultaneously implementation the same code M times with a various round-off error diffusion for each run;
- evaluating the common part of these results and to propound that this part is the same as the accurate result.

In practice, these different round-off error propagations are obtained in using random rounding mode. In fact, each result e of a FPA operation corresponding to a real number E is always bounded by two values E^- and E^+, each of them being so representative of the accurate result. The random rounding consists at the level of each FPA operation or assignment to choose as result randomly with an equal probability either E^- or E^+. Then when the same code is performed, M times with a computer using this random rounding, M results $E_i, i = 1, ..., M$, are obtained. It has been proved in that, under some assumptions, these M results belong to a quasi-Gaussian distribution focused on the accurate result e. So, as a matter of fact, to take into view the average value E_{ave} of the E_i as the calculated result, and using Student test, it is possible to obtain a confidence interval of E with a probability $(1-\theta)$ and then to evaluate the estimate number of exact significant digits of $\overline{E}$ by

$$C_{E_{ave}} = \log_{10}\left(\frac{\sqrt{M}|E_{ave}|}{\tau_\theta s}\right), \tag{2.1}$$

where $E_{ave} = (1/M)\sum_{i=1}^{M} E_i$, and $s^2 = \dfrac{1}{M-1}\sum_{i=1}^{M}(E_i - E_{ave})^2$.
s is the standard deviation and τ_θ is the value of the Student distribution for $M-1$

[1]Control et estimation stochastique des arrondis de calculs.
[2]Control of Accuracy and Debugging for Numerical Applications

degrees of freedom and a probability level $1-\theta$. In practice $M=3$, $\theta=0.05$ and then $\tau_\theta=4.4303$.

Definition 2.1. Each result presented by the CESTAC method is an informatical zero shown with @.0 iff one of the following two conditions be met:

1) $E_i=0, i=1,2,...,M.$ 2) $C_{E_{ave}}\leq 0.$

In this case, E_{ave} has no significant digit.

Definition 2.2. Let P and Q be M-samples provided by the CESTAC method, discrete stochastic equality denoted by $s^=$ is defined as follows:
$Ps^=Q$ if $P-Q=@.0$.

The Discrete Stochastic Arithmetic (DSA) is the association of the CESTAC method, the concept of computational zero and the discrete stochastic relations. Based on the DSA, it is possible to control the run of a scientific code, to indicate the numerical instabilities and the validation of results in a program. The two main features of the CESTAC method include:

- The random rounding, which contains in fathering E^- and E^+ and in choosing randomly one of the two.
- The manner to perform the M runs of a code.

With IEEE arithmetic and the possibilities of ADA, C++, and Fortran to create new structures and to overload the operators it is easy to implement the CESTAC method.

It is absolutely necessary to detect, during the run of a code, the emergence of @.0 for controlling the validity of the CESTAC method. To achieve this it suffices to use the synchronous implementation which consists of performing each arithmetic operation M times with the random rounding before performing the next. Thus, for each numerical result we have M samples, from which the number of the exact significant digits of the average value, considered as the computed result, is estimated. The applying of the CESTAC method in a scientific program has the following advantages:

(1) The accuracy of any numerical result is estimated, during the performance of a code.
(2) The numerical instabilities are detected and the branching is checked.
(3) Unnecessary iterations are eliminated which the FPA is not able to distinguish them. In some cases, the termination criterion of iterative methods is not suitable so that the implementation of the algorithm is continued without improvement in the accuracy of the result. In the SA, instead of the termination criterion, a criterion that directly reflects the mathematical condition, is replaced, that must be satisfied by the solution.
(4) It is able to find the optimal step of the iterative methods, which after this step, the accuracy of the result does not increase or maybe decrease, because of the rounding error accumulation.
(5) It is an effective and powerful tool that helps us to achieve the validation of scientific programs and gives them reliability.

3. Main idea

Let the function u in Eq.(1.1) is approximated by:

$$u \simeq w = \sum_{k=1}^{N} \lambda_k \psi_k, \tag{3.1}$$

where λ_k's are unknown coefficients[7]. We consider the MQ-RBF and GA-RBF functions. The function ψ represents a radial basis function, where $\psi_k = \sqrt{\epsilon^2 + r_k^2}$ or $\psi_k = e^{-\epsilon^2 r_k^2}$, that in one-dimensional $r_k^2 = (x - x_k)^2$ and in the two-dimensional $r_k^2 = (x - x_k)^2 + (y - y_k)^2$. The set of N distinct points are divided into two parts. Assume that there are N_I centers in the interior of the domain $\Omega/\partial\Omega$ and N_B centers on the boundary $\partial\Omega$. For the interior centers and fixed point $x^* \in \mathbb{R}^d$, we apply the operator $\mathcal{L}$ to the RBF interpolation as

$$\mathcal{L}u(x_i^*) = \sum_{k=1}^{N} \lambda_k \mathcal{L}\psi_k(x_i^*) = f(x_i^*), i = 1, 2, ..., N_I,$$

for the boundary centers, we have

$$\mathcal{B}u(x_i^*) = \sum_{k=1}^{N} \lambda_k \mathcal{B}\psi_k(x_i^*) = g(x_i^*), i = N_I + 1, ..., N.$$

An interpolation matrix can be expressed as

$$\begin{bmatrix} \mathcal{L}\psi \\ \mathcal{B}\psi \end{bmatrix} [\lambda] = \begin{bmatrix} f \\ g \end{bmatrix} \Longrightarrow A\lambda = q. \tag{3.2}$$

Since the matrix A is the nonsingular matrix [7], therefore we use the LU factorization to solve the system (3.2) and obtain λ_k unknown coefficients. Also, the condition number of matrix A is computed on a given norm via the following relation:

$$Cond(A) = \|A\| \left\|A^{-1}\right\|. \tag{3.3}$$

Let meshless points $\Xi_k = \{x_k\}_{k=1}^N$ or $\Xi_k = \{(x_k, y_k)\}_{k=1}^N$ be a given set of distinct points in domain Ω in $\mathbb{R}^d$, then the infinite norm error(τ), the root mean square (RMS) error and the relative root mean square(RES) error are as follows:

$$\begin{aligned} \tau &= \|u - w\|_\infty \simeq \max_{1 \le k \le N} |u(\Xi_k) - w(\Xi_k)|, \\ RMS(u, w) &= \sqrt{\frac{1}{N} \sum_{k=1}^{N} (u(\Xi_k) - w(\Xi_k))^2}, \\ RES(u, w) &= \frac{\sum_{k=1}^{N} (u(\Xi_k) - w(\Xi_k))^2}{\sum_{k=1}^{N} (u(\Xi_k))^2}. \end{aligned} \tag{3.4}$$

where w is defined by (3.1).

3.1. **Algorithms in CADNA library.** The CADNA library is a tool to implement the CESTAC method automatically. The first goal of this library is the estimation of the accuracy of each computed result. The CADNA detects numerical instabilities (informatical zero) during the run of the program[23]. The CADNA works on Fortran or $C++$ codes on the Linux operating system[16, 17]. When a result is a stochastic zero(i.e. is insignificant), the symbol @.0 is printed. For more details about this library we refer the reader to *" http://www-pequan.lip6.fr/cadna "*.

The following algorithms are proposed to solve a differential equation via RBF-meshless method based on the SA. Suppose w^i, w^{i-1} are the approximate values of u in two successive iterations obtained from the MQ-RBF and the GA-RBF method at the meshless points $\Xi_k = \{x_k\}_{k=1}^N$ or $\Xi_k = \{(x_k, y_k)\}_{k=1}^N$. If the MQ-RBF or GA-RBF method is used in order to estimate $u(\Xi_k)$ then, for suitable choice of N and ϵ, the number of common significant digits between $w^i(\Xi_k)$ and $w^{i-1}(\Xi_k)$ are almost equal to the number of common significant digits between $u(\Xi_k)$ and $w^i(\Xi_k)$. Therefore, if the CESTAC method is applied then, the computations of the sequence $w^i(\Xi_k)$'s are stopped when for an index like N_{opt}, ϵ_{opt}, $\left\|w^i - w^{i-1}\right\|_\infty = @.0$ or $RMS(w^i, w^{i-1}) = @.0$ or $RES(w^i, w^{i-1}) = @.0$. Thus the termination criterion, we consider the infinity error norm, RMS and RES to be an informatical zero denoted by @.0. The outputs of all algorithms are N, ϵ, $w^i(\Xi_k)$, $\left\|w^i - w^{i-1}\right\|_\infty$, RMS, RES and $Cond(A)$.
In the following algorithm, ϵ considered as a constant value and in an iterative process by increasing N, the N_{opt} is obtained.

Algorithm 3.1. *(finding the N_{opt} with $\{\Xi_k\}_{k=1}^N$ and fixed shape parameter)*
step1-Let $i = 1$, choose a fixed ϵ and arbitrary N
step2- Compute $w^i(\Xi_k), k = 1, 2, ..., N$ based on (3.1)
step3- If $\left\|w^i - w^{i-1}\right\|_\infty = @.0$ (or $RMS(w^i, w^{i-1}) = @.0$ or $RES(w^i, w^{i-1}) = @.0$) on bases (3.4)) then stop
step4- Else $N = N + 1, i = i + 1$ and goto step 2.
step5- EndIf.

In two following algorithms, N is fixed and in an iterative process by changing ϵ, the ϵ_{opt} is obtained.

Algorithm 3.2. *(finding the ϵ_{opt} for MQ-RBF with the $\{\Xi_k\}_{k=1}^N$ and fixed N)*
step1- Let $i = 1$, choose a fixed N, $0 < \delta \ll 1$ and arbitrary ϵ
step2- Compute $w^i(\Xi_k), k = 1, 2, ..., N$ based on (3.1)
step3- If $\left\|w^i - w^{i-1}\right\|_\infty = @.0$ (or $RMS(w^i, w^{i-1}) = @.0$ or $RES(w^i, w^{i-1}) = @.0$) on bases (3.4)) then stop
step4- Else $\epsilon = \epsilon + \delta, i = i + 1$ and goto step 2.
step5- EndIf.

Algorithm 3.3. *(finding the ϵ_{opt} for GA-RBF with the $\{\Xi_k\}_{k=1}^N$)*
step1- Let $i = 1$, choose a fixed N, $0 < \delta \ll 1$ and arbitrary small ϵ
step2- Compute $w^i(\Xi_k), k = 1, 2, ..., N$ based on (3.1)
step3- If $\left\|w^i - w^{i-1}\right\|_\infty = @.0$ (or $RMS(w^i, w^{i-1}) = @.0$ or $RES(w^i, w^{i-1}) = @.0$) on bases (3.4) then stop

step4- Else $\epsilon = \epsilon - \delta, i = i + 1$ *and goto step 2.*
step5- EndIf.

In the step 1 of algorithms 2 and 3, the initial choice ϵ is optional.
Note that for calculating approximate solution at the arbitrary point like $\xi \in \Omega$ or (ξ, η) in two-dimensional , we use the stopping criterion $\left|w^i(\xi) - w^{i-1}(\xi)\right| = @.0$ or $\left|w^i((\xi,\eta)) - w^{i-1}((\xi,\eta))\right| = @.0$, in two successive iterations.

4. Numerical Examples

In this section, three sample differential equations are considered to be solved by the RBF-meshless method based on the algorithms 1, 2 and 3. All the numerical experiments have been computed in double precision by C++ codes and CADNA library in Linux machine.

Examples 4.1. *Consider the steady convection-diffusion problem*

$$\begin{aligned} &u_x - u_{xx} = \pi^2 \sin(\pi x) + \pi \cos(\pi x), \qquad x \in (0,1), \\ &u(0) = 0, \qquad u(1) = 1. \end{aligned} \tag{4.1}$$

The exact solution of Eq. (4.1) is $u(x) = \sin(\pi x) + \dfrac{e^x - 1}{e - 1}$.

This problem was proposed and solved in [8, 10, 11].
To solve Eq.(4.1) by RBF-meshless method, the following meshless points are chosen:

$$x_k = \sin\left(\frac{(k-1)\pi}{2(N-1)}\right), \ k = 1, 2, ..., N. \tag{4.2}$$

The main goal is to solve Eq. (4.1) and to find the optimal shape parameter and the optimal number of points. As far as the choice of the optimal shape parameter depends on the node points, so first we examine the numerical results at the point x^* like 0.5, then we consider the general case based on infinite norm error, RMS error, RES error. As seen in Figure 1, with successive implementation of algorithm 1, optimal number of the points in MQ-RBF method is obtained with range $0.1 < \epsilon < 6$ for solving Eq.(4.1) at the point $x = 0.5$. Truncation error in the case $\epsilon = 0.1$ is $0.15E-003$ and in the case $\epsilon = 6$ is $0.3E-002$, that if ϵ is selected outside of this range, truncation error gradually increases. In best situation, by choosing $N_{opt} = 21, \epsilon = 0.52$ truncation error in $N = 20$ is $0.5E-006$ and by choosing $N_{opt} = 11, \epsilon = 2.02$ truncation error in $N = 10$ is $0.7E-006$. Therefore, the best range for ϵ in equation (4.1) is $0.1 < |\epsilon| < 6$. So, by implementing algorithm 1 alternatively, the optimal numbers of the points with range $0.2 < \epsilon < 7$ in solving Eq.(4.1) by using GA-RBF method at the point $x = 0.5$ is obtained. The results are shown in Figure 2. Truncation error in the case $\epsilon = 0.2$ is $0.479E-002$ and in the case $\epsilon = 7$ is $0.2E-004$. But in the outside of this range, truncation error gradually increases or numerical instability occurs. For example, in the case $N = 7, \epsilon = 0.14$, according to Table 1 the notation @.0 is displayed in the column $u(0.5)$, which means the numerical instability.

FIGURE 1. $x = 0.5$, MQ-RBF

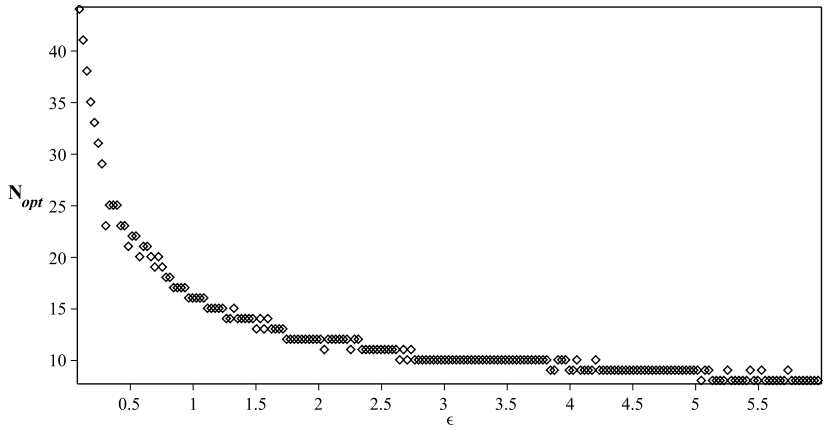

FIGURE 2. $x = 0.5$, GA-RBF

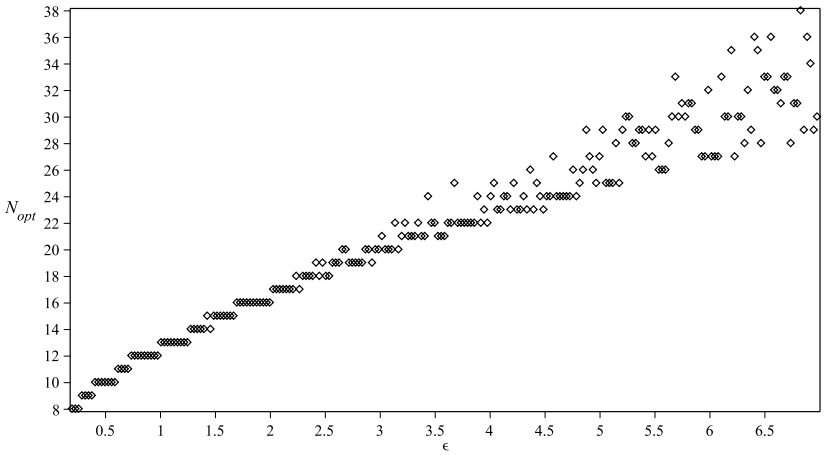

TABLE 1. Numerical results of Example 4.1

GA-RBF, $x = 0.5$, $\epsilon = 0.14$				
N	$u(0.5)$	$\lvert u(0.5) - w^i(0.5)\rvert$	$\lvert w^i(0.5) - w^{i-1}(0.5)\rvert$	$Cond(A)$
5	0.13819E+001	0.439E-002	0.13819E+001	0.87644339E+010
6	0.1376E+001	0.9E-003	0.5E-002	0.17593E+014
7	@.0	@.0	@.0	0.50E+017

In the GA-RBF method, by choosing $N = 15, \delta = 0.03$ and applying algorithm 3, we find the optimal shape parameter $\epsilon_{opt} = 2.02$ and in the MQ-RBF, by choosing

$N = 23, \delta = 0.03$ and applying algorithm 2, it is calculated $\epsilon_{opt} = 0.36$. In order to compare these two methods, the values τ, RMS and RES are shown in Figure 3 and Figure 4.

FIGURE 3

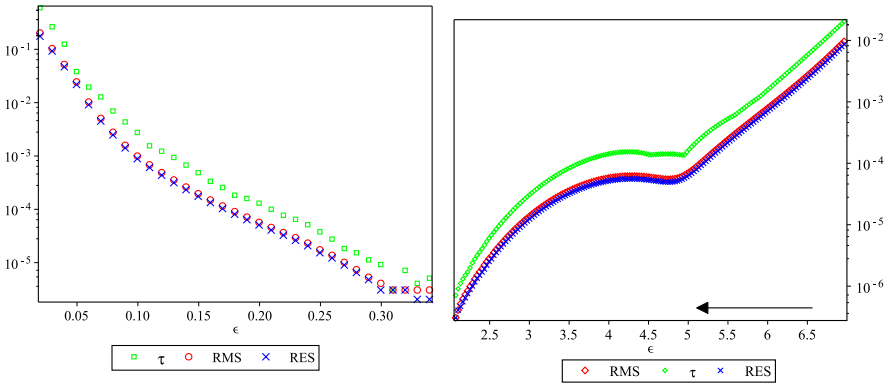

(a) ϵ_{opt}=0.36, N=23, MQ (b) ϵ_{opt}=2.02, N=15, GA

The condition numbers of the matrix A product of the MQ-RBF and GA-RBF methods are shown in Figure 5 and Figure 5.

FIGURE 4

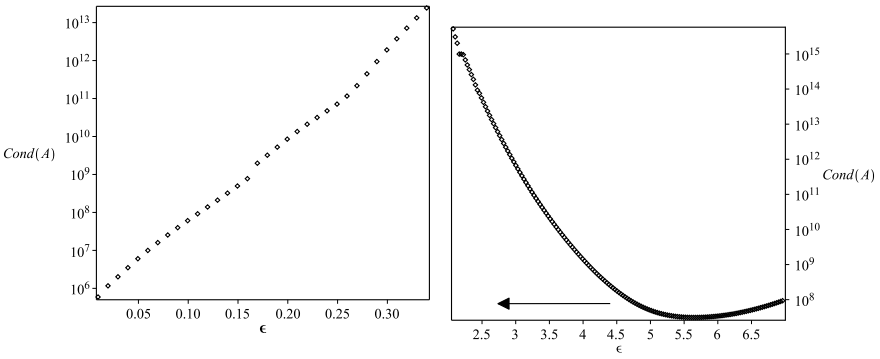

(a) ϵ_{opt}=0.36, N=23, MQ (b) ϵ_{opt}=2.02, N=15, GA

The numerical results of Example 1 for MQ-RBF, is given in Table 2. In this table, by choosing fixed $\epsilon = 0.61$ optimal number of the point $N_{opt} = 20$ is obtained. In the last column, condition number of the matrix A is shown as $Cond(A) = @.0$ at optimal step. This means that, by increasing N, condition number of matrix A is

TABLE 2. Numerical results of Example 4.1

MQ-RBF, $x = 0.5, \epsilon = 0.61$				
N	$u(0.5)$	$\lvert u(0.5) - w^i(0.5)\rvert$	$\lvert w^i(0.5) - w^{i-1}(0.5)\rvert$	$Cond(A)$
5	0.1360100505853E+001	0.17440162944E-001	-	0.1045687714775E+004
6	0.1338901684992E+001	0.38638983805E-001	0.21198820860E-001	0.1174472550529E+005
7	0.1377300046137E+001	0.240622660E-003	0.38398361144E-001	0.237171865855E+005
8	0.137766960951E+001	0.12894071E-003	0.36956337E-003	0.24046608672E+006
9	0.137762843490E+001	0.87766104E-004	0.41174609E-004	0.81758887703E+006
⋮	⋮	⋮	⋮	⋮
15	0.137751896E+001	0.2169E-004	0.1068E-004	0.16968E+012
16	0.137752511E+001	0.1555E-004	0.614E-005	0.1837E+013
17	0.13775309E+001	0.97E-005	0.57E-005	0.132E+014
18	0.1377533E+001	0.72E-005	0.25E-005	0.14E+015
19	0.1377535E+001	0.4E-005	0.2E-005	0.11E+016
20	0.137753E+001	@.0	@.0	@.0

TABLE 3. Numerical results of Example 4.1

MQ-RBF, $x = 0.5$, $N = 20$				
ϵ	$u(0.5)$	$\lvert u(0.5) - w^i(0.5)\rvert$	$\lvert w^i(0.5) - w^{i-1}(0.5)\rvert$	$Cond(A)$
0.10	0.1377608600E+001	-	-	0.1095701648E+008
0.13	0.137516487E+001	0.2375798E-002	0.2443729E-002	0.29869417032E+008
0.16	0.137340314E+001	0.4137525E-002	0.176172E-002	0.8092274576E+008
⋮	⋮	⋮	⋮	⋮
0.37	0.1377703E+001	0.162E-003	0.309E-003	0.1182E+013
0.40	0.1377608E+001	0.67E-004	0.95E-004	0.3724E+013
0.43	0.1377570E+001	0.29E-004	0.37E-004	0.1232E+014
0.46	0.1377552E+001	0.12E-004	0.17E-004	0.407E+014
0.49	0.1377544E+001	0.3E-005	0.86E-005	0.13E+015
0.52	0.137754E+001	0.28E-005	0.4E-005	0.42E+015
0.55	0.13775379E+001	0.26E-005	0.2E-005	0.13E+016
0.58	0.1377537E+001	0.35E-005	0.8E-006	0.4E+016
0.61	0.137753E+001	0.3E-005	@.0	0.1E+017

insignificant.

By fixing the number $N = 20$, according to Table 3 the optimal shape parameter $\epsilon_{opt} = 0.61$ is obtained.

Numerical results of the Eq. (4.1) by using GA-RBF meshless method at the point $x = 0.5$ by the implementing algorithms 2, 3, with $\delta = 0.03$ are shown in the Tables 4 and 5 respectively.

In the present method, the optimal shape parameter is obtained from an iterative process. According to the type of nodal points in the choice of the shape parameter, the method presented in [8, 10, 11] and the present approach is completely different. Therefore, the approximate solution is compared with the exact solution. We can be see a comparison between the exact solution and approximate solutions in Figure 6, that for MQ-RBF $N = 23, \epsilon_{opt} = 0.36$ and in the GA-RBF $N = 15, \epsilon_{opt} = 2.02$ is

TABLE 4. Numerical results of Example 4.1

GA-RBF, $x = 0.5$, $N = 15$				
ϵ	$u(0.5)$	$\lvert u - w^i \rvert$	$\lvert w^i - w^{i-1} \rvert$	$Cond(A)$
3.00	0.137770686E+001	0.16619E-003	-	0.88406E+012
2.97	0.13776911E+001	0.1504E-003	0.157E-004	0.1109E+013
2.94	0.137767659E+001	0.13592E-003	0.145E-004	0.13978E+013
⋮	⋮	⋮	⋮	⋮
2.73	0.13776030E+001	0.6235E-004	0.788E-005	0.76877E+013
2.70	0.13775958E+001	0.5520E-004	0.715E-005	0.994E+013
2.67	0.137758940E+001	0.4873E-004	0.646E-005	0.1290E+014
⋮	⋮	⋮	⋮	⋮
2.52	0.13775656E+001	0.249E-004	0.37E-005	0.505E+014
2.49	0.13775622E+001	0.2161E-004	0.33E-005	0.673E+014
2.46	0.137755931E+001	0.1865E-004	.296E-005	0.901E+014
⋮	⋮	⋮	⋮	⋮
2.22	0.13775456E+001	0.497E-005	0.98E-006	0.1E+016
2.19	0.13775448E+001	0.413E-005	0.838E-006	0.1E+016
2.16	0.13775440E+001	0.34E-005	0.72E-006	0.2E+016
2.13	0.1377543E+001	0.28E-005	0.5E-006	0.2E+016
2.10	0.1377542E+001	0.20E-005	0.5E-006	0.4E+016
2.07	0.1377542E+001	0.18E-005	0.4E-006	0.5E+016
2.04	0.1377542E+001	0.1E-005	@.0	0.8E+016

TABLE 5. Numerical results of Example 4.1

GA-RBF, $x = 0.5$, $\epsilon = 2.04$				
N	$u(0.5)$	$\lvert u(0.5) - w^i(0.5) \rvert$	$\lvert w^i(0.5) - w^{i-1}(0.5) \rvert$	$Cond(A)$
5	0.1395488710116E+001	0.17948041317E-001	-	0.1872125243342E+004
6	0.1336191141684E+001	0.413495271131E-001	0.592975684311E-001	0.5771636338915E+004
7	0.1384711165077E+001	0.71704962795E-002	0.48520023392E-001	0.215714784845E+005
8	0.138017982618E+001	0.263915738E-002	0.4531338896E-002	0.259176319219E+006
9	0.137882831546E+001	0.128764667E-002	0.135151071E-002	0.3439990104E+007
10	0.13778782059E+001	0.3375371E-003	0.95010954E-003	0.87175544E+008
11	0.1377669063E+001	0.128394E-003	0.2091424E-003	0.2574423E+010
12	0.137757363E+001	0.32969E-004	0.95425E-004	0.914767E+011
13	0.137755532E+001	0.1465E-004	0.1831E-004	0.3727E+013
14	0.1377543E+001	0.2E-005	0.12E-004	0.170E+015
15	0.1377542E+001	0.1E-005	0.1E-005	0.8E+016
16	0.137754E+001	@.0	@.0	@.0

selected.

Examples 4.2. *We consider a two-dimensional Poisson problem, defined by:*[26, 31]

$$\begin{aligned} &\nabla^2 u(x,y) = (\lambda^2 + \mu^2) e^{\lambda x + \mu y}, && (x,y) \in \Omega = [0,1], \\ &u(x,y)|_{\partial\Omega} = g(x,y), && (x,y) \in \partial\Omega, \end{aligned} \tag{4.3}$$

where ∇ *is the Laplace operator. The exact solution of Eq. (4.3) is as follows:*

$$u(x,y) = e^{\lambda x + \mu y}.$$

FIGURE 5. A comparison of exact and approximate solutions (Blue points : GA-RBF, $N = 15, \epsilon = 2.02$ Red points : MQ-RBF, $N = 23, \epsilon = 0.36$)

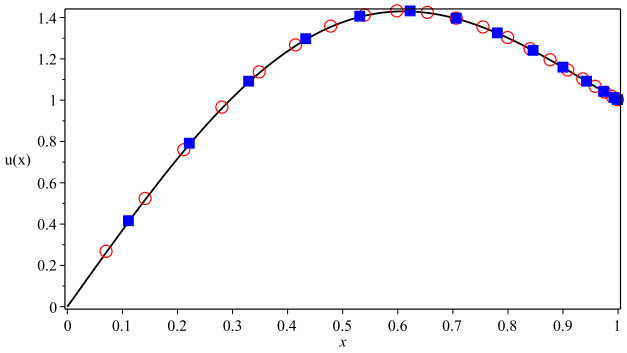

For boundary conditions have

$$\begin{aligned} g(0, y_i) &= e^{\mu y_i}, \qquad i = 1, 2, ..., N_1, \\ g(1, y_i) &= e^{\lambda + \mu y_i}, \qquad i = 1, 2, ..., N_2, \\ g(x_i, 0) &= e^{\lambda x_i}, \qquad i = 1, 2, ..., N_3, \\ g(x_i, 1) &= e^{\lambda x_i + \mu}, \qquad i = 1, 2, ..., N_4, \end{aligned}$$

where $N_B = N_1 + N_2 + N_3 + N_4$ total number of boundary points.
In solving of Eq. (4.3), the $N_B = 20$ boundary points are used. Also, we present irregular grid points $\{(x_k, y_k)\}_{k=1}^{N}$ in using the RBF-meshless method. Irregular grid points are created by code $rand()$ in the C++. Number $N = 48$ irregular grid points for MQ-RBF method are selected as illustrated in Figure 7.

In Figure 8, when $\lambda = 1, \mu = 2$, we can see a comparison of the exact solution and approximation solutions, the numerical results with optimal choice $N = 48, \epsilon = 1.11$ for MQ-RBF and $N = 28, \epsilon = 0.68$ for GA-RBF is obtained by the CESTAC method. As well as for comparison, the method proposed in [31] under a domain the unit circle with double precision, for $N = 20, 30, 60$ optimal shape parameters and RMS errors are obtained $\epsilon = 0.035, 0.1, 0.2$ and $3.1E-2, 2.9E-3, 4.8E-4$, respectively. By repeating the execution of algorithm 1 and selecting ϵ in the interval $0.75 < |\epsilon| < 2.9$, optimal number of the points is calculated by using MQ-RBF meshless method at the point $(0.5, 1)$. These results can be seen in Figure 9. In the interval $0.75 < |\epsilon| < 2.9$, truncation error in the lowest and highest values are $0.6E-006$ and $0.1E-002$, respectively. In outside of this interval, the error is increasing gradually. Of the best choices are $N_{opt} = 63, \epsilon = 0.73$ and $N_{opt} = 27, \epsilon = 1.65$ that truncation error is elmost $0.6E-006$. When $\epsilon = 0.72, N = 122$ numerical instability happens, that in the second column of the Table 6 it can be seen with the symbol @.0. To solve the Eq. (4.3) by GA-RBF meshless method at the point $(0.5, 1)$, when $0.4 < |\epsilon| < 1.94$ optimal number of points is obtained by successive implementation of algorithm 1. These results can be seen in Figure 10. For example, in the case $\epsilon = 2.32, N = 100$

FIGURE 6. N=48, irregular grid

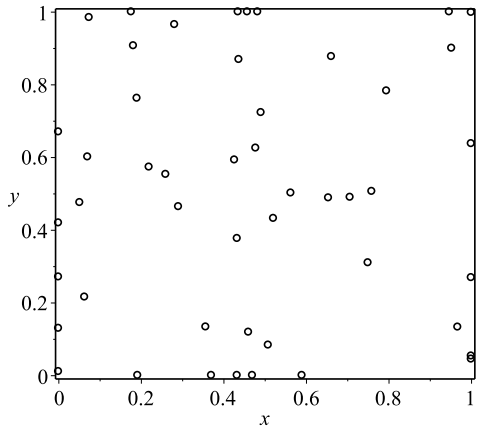

FIGURE 7. A comparison of exact and approximate solutions (Red points: MQ-RBF, N=48, $\epsilon = 1.11$. Blue points: GA-RBF, N=28, $\epsilon = 0.68$.)

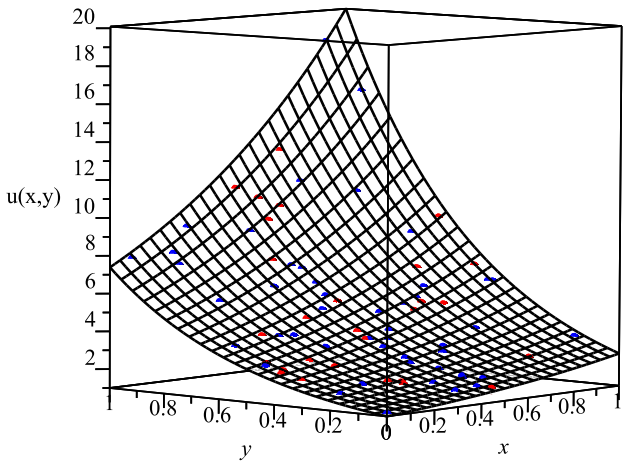

as shown in Table 7, numerical instability is observed. The curve of the errors for MQ-RBF method is plotted in Figure 11. By implementation of the algorithm 2 with $\delta = 0.03$ and the fixed number $N = 48$, the optimal shape parameter $\epsilon_{opt} = 1.8$ is obtained. Also, the errors of the GA-RBF method, is shown in Figure 11 and with

FIGURE 8. $x = 0.5, y = 1$, MQ-RBF

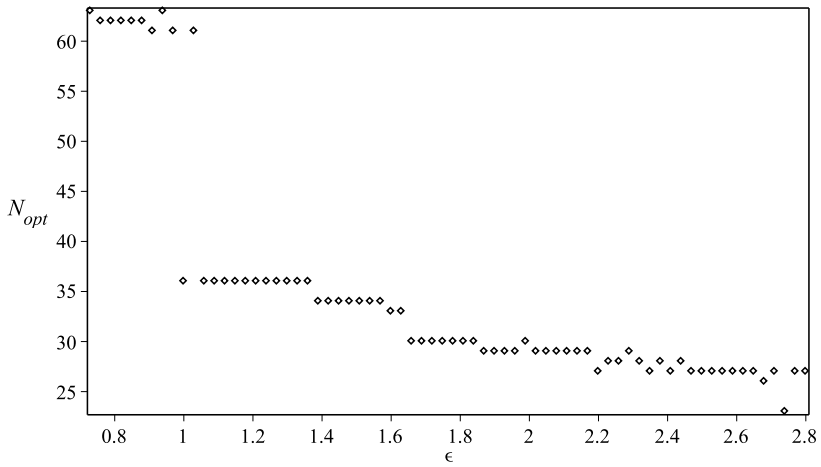

FIGURE 9. $x = 0.5, y = 1$, GA-RBF

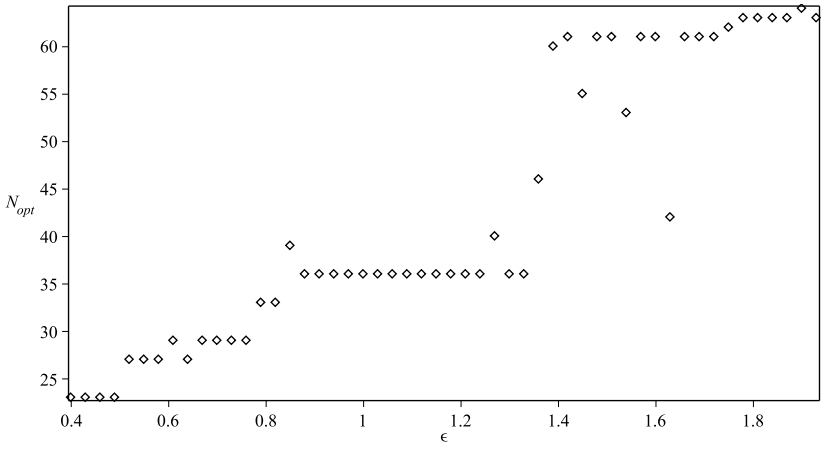

fixed number $N = 28$, the optimal shape parameter $\epsilon_{opt} = 0.68$ is obtained. So, in Figures 12 and 12, condition number of the matrix A can be observed. It can be seen in Table 8, by algorithm 1, the numerical results of the Eq.(4.3) by using MQ-RBF meshless method at the point $(0.5, 1)$ when $\epsilon = 1.8$, the optimal number of point $N_{opt} = 29$ is obtained. Also, in Table 9, The number of points $N = 48$ is fixed and the optimal value of $\epsilon_{opt} = 1.11$ is obtained by using algorithm 2 with $\delta = 0.03$.

By applying GA-RBF meshless method to solve the Eq. (4.3) at the point $(0.5, 1)$, the numerical results can be seen in Tables 10 and 11. In this way, by the algorithms

Table 6. Numerical results of Example 4.2

MQ-RBF, $\lambda = 1, \mu = 2, \delta = 0.03$, $N = 122$				
ϵ	$u(0.5, 1)$	$\lvert u - w^i \rvert$	$\lvert w^i - w^{i-1} \rvert$	$Cond(A)$
0.60	0.1217804E+002	0.4449E-002	-	0.22775E+014
0.63	0.1218256E+002	0.6E-004	0.451E-002	0.6794E+014
0.66	0.122034E+002	0.209E-001	0.208E-001	0.2407E+015
0.69	0.1228E+002	0.10E+000	0.81E-001	0.120E+016
0.72	@.0	@.0	@.0	@.0

Table 7. Numerical results of Example 4.2

GA-RBF, $\lambda = 1, \mu = 2$, $\epsilon = 2.32$				
N	$u(0.5, 1)$	$\lvert u - w^i \rvert$	$\lvert w^i - w^{i-1} \rvert$	$Cond(A)$
21	0.130629871E+002	0.88049322	-	0.17883362E+010
22	0.121714675E+002	0.1102645E-001	0.89151968	0.46001900E+009
⋮	⋮	⋮	⋮	⋮
98	0.12245E+002	0.629E-001	0.682E-001	0.3935E+015
99	0.11E+002	0.1E+001	0.1E+001	0.1E+017
100	@.0	@.0	@.0	@.0

Table 8. Numerical results of Example 4.2

MQ-RBF,$(x, y) = (0.5, 1), \lambda = 1, \mu = 2$, $\epsilon = 1.8$				
N	$u(0.5, 1)$	$\lvert u - w^i \rvert$	$\lvert w^i - w^{i-1} \rvert$	$Cond(A)$
21	0.1204E+002	0.141E+000	-	0.28E+015
22	0.121907E+002	0.829E-002	0.150E+000	0.807E+014
⋮	⋮	⋮	⋮	⋮
25	0.1218386E+002	0.136E-002	0.2685E-002	0.1306E+014
26	0.12182515E+002	0.21E-004	0.134E-002	0.83E+015
27	0.12182487E+002	0.59E-005	0.27E-004	0.7662E+014
28	0.12182479E+002	0.14E-004	0.88E-005	0.187E+015
29	0.121824E+002	@.0	@.0	0.15E+016

Table 9. Numerical results of Example 4.2

MQ-RBF, $(x, y) = (0.5, 1), \lambda = 1, \mu = 2, \delta = 0.03$, $N = 48$				
ϵ	$u(0.5, 1)$	$\lvert u - w^i \rvert$	$\lvert w^i - w^{i-1} \rvert$	$Cond(A)$
0.30	0.1217726748E+002	0.5226479E-002	-	0.3707078E+011
0.33	0.1217397509E+002	0.8518864E-002	0.329238E-002	0.560850511E+010
⋮	⋮	⋮	⋮	⋮
0.78	0.12182070E+002	0.423E-003	0.558E-003	0.31543E+013
0.81	0.12182229E+002	0.264E-003	0.159E-003	0.295645E+013
⋮	⋮	⋮	⋮	⋮
0.99	0.1218243E+002	0.56E-004	0.1E-004	0.9225E+013
1.02	0.1218244E+002	0.46E-004	0.9E-005	0.1208E+014
1.05	0.1218245E+002	0.38E-004	0.7E-005	0.1589E+014
1.08	0.1218246E+002	0.3E-004	0.6E-005	0.2093E+014
1.11	0.1218246E+002	0.2E-004	@.0	0.2759E+014

FIGURE 10

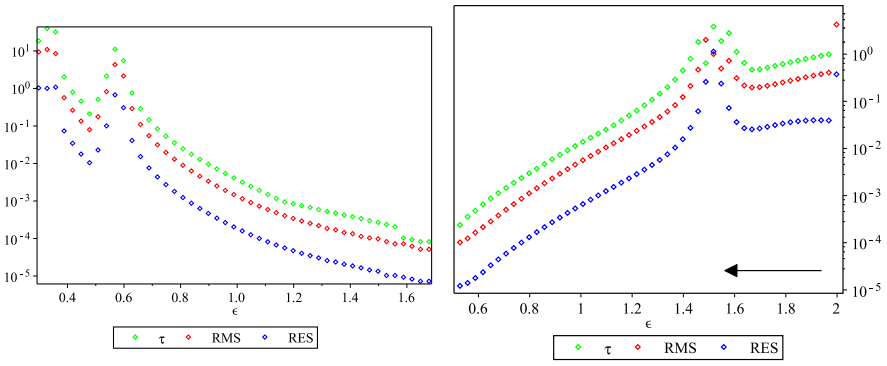

(a) $\epsilon_{opt} = 1.8$, N=48, MQ (b) $\epsilon_{opt} = 0.68$, N=28, GA

FIGURE 11

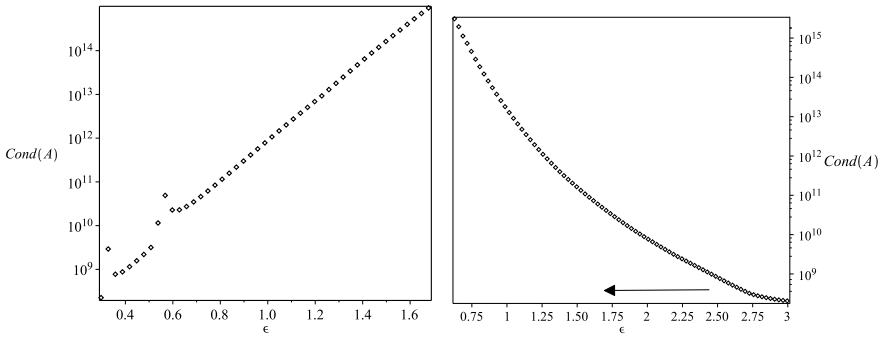

(a) $\epsilon_{opt} = 1.8$, N=48, MQ (b) $\epsilon_{opt} = 0.68$, N=28, GA

1 and 3, when ϵ is a constant value, the optimal N_{opt} is obtained and when N is considered to be fixed the optimal ϵ_{opt} is found.

Examples 4.3. *Consider the cubic Duffing oscillator equation*[36, 38]

$$\begin{aligned} &\frac{d^2y}{dt^2} + ky + \sigma y^3 = |k-1|\, cost, \qquad 0 \le t \le T, \\ &y(0) = 0,\ y'(0) = 0. \end{aligned} \tag{4.4}$$

The solution depends on the two dimensionless parameters k and σ.

TABLE 10. Numerical results of Example 4.2

GA-RBF, $(x,y)=(0.5,1), \lambda=1, \mu=2, \delta=0.03, N=28$				
ϵ	$u(0.5,1)$	$\lvert u-w^i\rvert$	$\lvert w^i-w^{i-1}\rvert$	$Cond(A)$
3.00	0.121880666463E+002	0.557268566E-002	-	0.223352853E+009
2.97	0.121863762037E+002	0.388224302E-002	0.16904426E-002	0.229478285E+009
⋮	⋮	⋮	⋮	⋮
2.40	0.121817150944E+002	0.77886628E-003	0.5445592E-004	0.136622222E+010
2.37	0.121817675503E+002	0.72641038E-003	0.5245590E-004	0.155101875E+010
⋮	⋮	⋮	⋮	⋮
1.56	0.121823916335E+002	0.1023272E-003	0.81361E-005	0.1130702E+012
1.53	0.12182399279E+002	0.946816E-004	0.76455E-005	0.138623E+012
⋮	⋮	⋮	⋮	⋮
0.75	0.121824885E+002	0.54E-005	0.1E-005	0.450E+015
0.72	0.121824893E+002	0.45E-005	0.8E-006	0.72E+015
0.69	0.12182490E+002	0.37E-005	0.8E-006	0.11E+016
0.66	0.12182490E+002	0.3E-005	0.7E-006	0.19E+016
0.63	0.12182491E+002	0.2E-005	@.0	0.3E+016

TABLE 11. Numerical results of Example 4.2

GA-RBF, $(x,y)=(0.5,1), \lambda=1, \mu=2, \epsilon=0.68$				
N	$u(0.5,1)$	$\lvert u-w^i\rvert$	$\lvert w^i-w^{i-1}\rvert$	$Cond(A)$
21	0.121757E+002	0.674E-002	-	0.641E+014
22	0.12183924E+002	0.1430E-002	0.817E-002	0.703E+014
⋮	⋮	⋮	⋮	⋮
25	0.12182720E+002	0.226E-003	0.498E-003	0.5329E+014
26	0.12182489E+002	0.46E-005	0.230E-003	0.14E+016
27	0.1218249E+002	0.1E-005	0.2E-005	0.148E+015
28	0.12182490E+002	0.35E-005	@.0	0.14E+016

To solve Eq.(4.4) by RBF-meshless method, the following meshless points are chosen:

$$t_k = \sin\left(\frac{(k-1)\pi}{2(N-1)}\right), \quad k=1,2,...,N. \tag{4.5}$$

First for case $k=30, \sigma=0$ and then cases $k=30, \sigma=0.1$ and $k=2, \sigma=0.1$, we illustrate this example.

In the case $k=30, \sigma=0$, by using RBF-meshless methods and applying algorithms 2 and 3, numerical results of the Eq. (4.4) for MQ-RBF method in $N=18, \epsilon_{opt}=0.76$ and GA-RBF method in $N=12, \epsilon_{opt}=1.25$ at $t\in[0,1]$ are shown in Table 12. Also in this table, the comparison of the present methods with differential transform method (DTM) [36] and pade approximation method[36] are represented. In the MQ-RBF method, by choosing $N=18, \delta=0.03$ and applying algorithm 2, we find the optimal shape parameter $\epsilon_{opt}=0.75$ and in the GA-RBF, by choosing $N=12, \delta=0.03$ and applying algorithm 3, it is calculated $\epsilon_{opt}=1.25$. In order to compare these two

TABLE 12. Numerical results of Example 4.3

Comparison of MQ, GA, DTM and P[5/4], $k = 30, \sigma = 0$				
t	MQ	GA	DTM	$P[5/4]$
0.1	0.1412	0.141291	0.1412914651	0.1412914643
0.2	0.5223	0.522414	0.5224158288	0.5224149658
0.3	1.0275	1.027643	1.027644677	1.027600040
0.4	1.5020	1.502171	1.502172577	1.501490977
0.5	1.7974	1.797478	1.797479057	1.792239670
0.6	1.81485	1.814876	1.814878675	1.789125527
0.7	1.5345	1.534514	1.534516826	1.442409794
0.8	1.0214	1.021326	1.021328053	0.7620357587
0.9	0.40632	0.406198	0.4062256777	0.1988810030
1.0	-0.1520	-0.152115	0.1518890375	1.365712996

methods, the values τ, RMS and RES are shown in Figure 13 and Figure 13. The

FIGURE 12

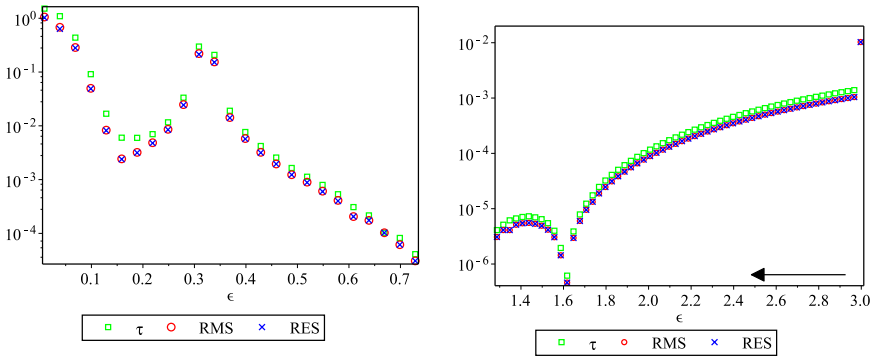

(a) MQ-RBF, N=18, $\epsilon_{opt} = 0.76, k = 30, \sigma = 0$.

(b) GA-RBF, N=12, $\epsilon_{opt} = 1.25, k = 30, \sigma = 0$.

condition numbers of the matrix A product of the MQ-RBF and GA-RBF methods are shown in Figure 14 and 14. Figure 15 shows a comparison of the present methods and DTM method in the case $k = 30, \sigma = 0$. In this figure, numerical results of MQ-RBF method and GA-RBF method with the implementation of the algorithms 2 and 3 by choosing $N = 18$ and $N = 12$ and finding $\epsilon_{opt} = 0.75$ and $\epsilon_{opt} = 1.25$ according to meshless points (4.5) are obtained, respectively.

In case $k = 30, \sigma = 0.1$ for the MQ-RBF method, by choosing $N = 15, \delta = 0.02$ and applying algorithm 2, we find the optimal shape parameter $\epsilon_{opt} = 0.82$ and in the GA-RBF, by choosing $N = 20, \delta = 0.02$ and applying algorithm 3, it is calculated $\epsilon_{opt} = 3.95$. In order to compare these two methods, the values τ, RMS and RES are shown in Figure 16 and 16.

However, in case $k = 2, \sigma = 0.1$ for the MQ-RBF method, by choosing $N = 15, \delta =$

FIGURE 13

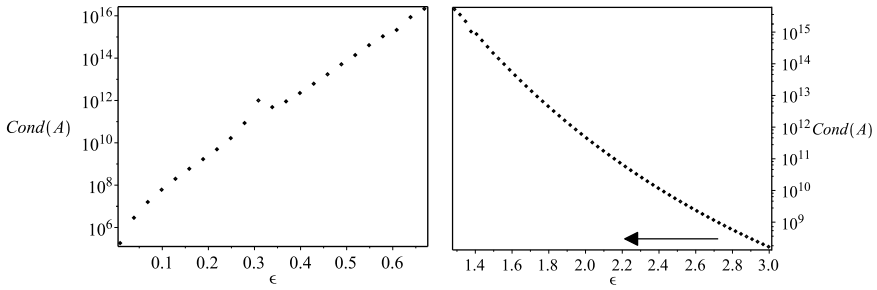

(a) MQ-RBF, N=18, $\epsilon_{opt} = 0.76, k = 30, \sigma = 0$. (b) GA-RBF, N=12, $\epsilon_{opt} = 1.25, k = 30, \sigma = 0$.

FIGURE 14. Comparison of RBF-meshless and DTM sulotions, $k = 30, \sigma = 0$.

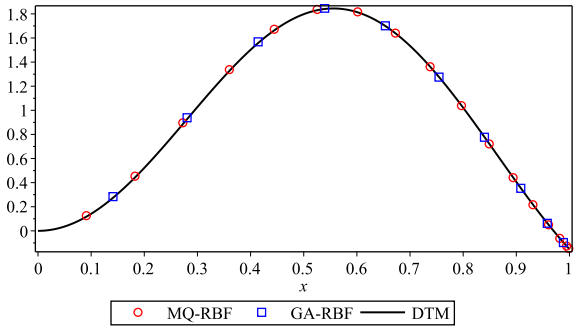

0.02 and applying algorithm 2, we find the optimal shape parameter $\epsilon_{opt} = 0.78$ and in the GA-RBF, by choosing $N = 22, \delta = 0.02$ and applying algorithm 3, it is calculated $\epsilon_{opt} = 4.80$. In order to compare these two methods, the values τ, RMS and RES are shown in Figure 17 and Figure 17.

In Figure 18 and 18, the comparison of the present methods with Laplace decomposition algorithm (LDA) [38] are represented in the cases $k = 30, \sigma = 0.1$ and $k = 2, \sigma = 0.1$, respectively. Figure 18 shows that numerical solutions to (4.4) for $\sigma = 0$ and $\sigma = 0.1$ are nearly identical in case of $k = 30$. However, Figure 18 shows that solutions corresponding to the same two values of σ differ considerably in case of $k = 2$.

5. Conclusion

We observed that the use of the CESTAC method and the CADNA library allows us to find the optimal ϵ_{opt} and N_{opt} of the MQ-RBF and GA-RBF meshless methods. Also, the results of the proposed algorithms are validated. Finding the optimal

FIGURE 15

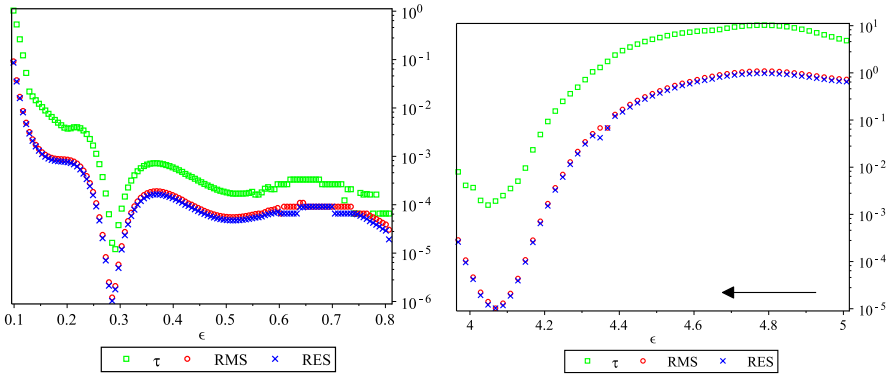

(a) MQ-RBF, N=15, $\epsilon_{opt} = 0.82, k = 30, \sigma = 0.1$ (b) GA-RBF, N=20, $\epsilon_{opt} = 3.95, k = 30, \sigma = 0.1$

FIGURE 16

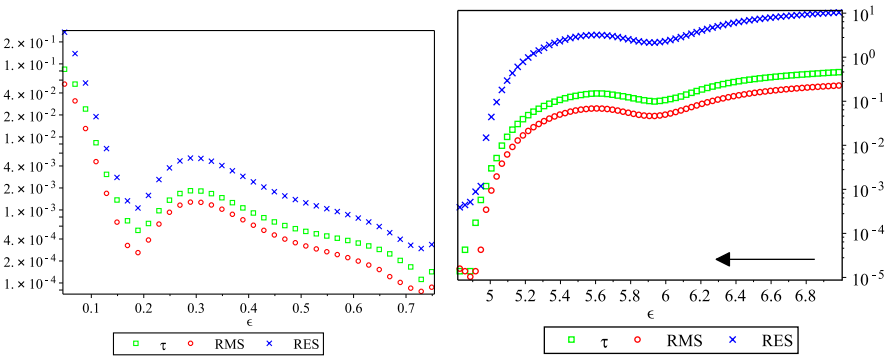

(a) $N = 15, \epsilon_{opt} = 0.78,\ k = 2, \sigma = 0.1$, MQ-RBF (b) $N = 22, \epsilon_{opt} = 4.80,\ k = 2, \sigma = 0.1$, GA-RBF

shape parameter, ϵ_{opt}, depends on: type of differential equation, type of meshless points(Ξ_k), number of meshless points (N), radial basis function ψ and computer precision. Consequently, it is suggested due to the numerical problems of the FPA, the SA is replaced to implement the algorithms of the RBF-meshless methods.

ACKNOWLEDGMENTS

The authors would like to thank the anonymous reviewers for their careful reading and constructive comments to improve the quality of this work and also the Islamic Azad university, central Tehran branch for their support during this research.

FIGURE 17. Comparison of RBF-meshless and LDA solutions

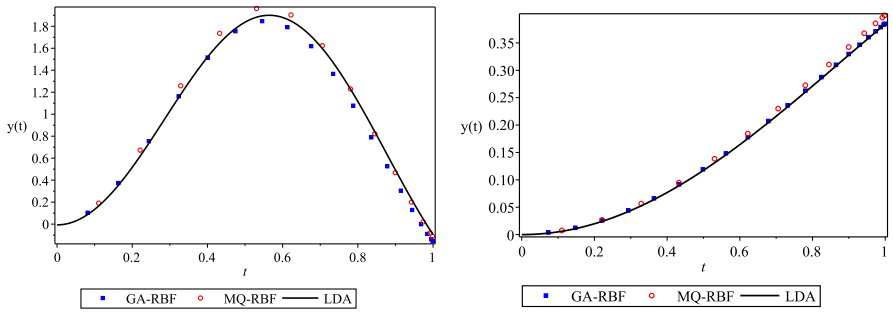

(a) $k = 30, \sigma = 0.1$ (b) $k = 2, \sigma = 0.1$

REFERENCES

[1] S. Abbasbandy and M. A. Fariborzi Araghi, *A Stochastic scheme for solving definite integrals,* Appl. Num. Math, *55*(2) (2005), 125-136.

[2] S. Abbasbandy and M. A. Fariborzi Araghi, *The use of the stochastic arithmetic to estimate the value of interpolation polynomial with optimal degree,* Appl. Numer. Math, *50*(3-4) (2004), 279-290.

[3] S. Abbasbandy and M. A. Fariborzi Araghi, *A reliable method to determine the ill-condition functions using stochastic arithmetic,* Southwest J. Pure Appl. Math, *1* (2002), 33-38.

[4] S. Abbasbandy and M. A. Fariborzi Araghi, *The valid implementation of numerical integration methods,* Far East J. Appl.Math, *8* (2002), 89-101.

[5] F. Afiatdoust and M. Esmaeilbeigi, *Optimal variable shape parameters using genetic algorithm for radial basis function approximation,* Ain Shams Eng J, *6*(2) (2015), 639-647.

[6] M. Amirfakhrian, M. Arghand, and E.J. Kansa, *A new approximate method for an inverse time-dependent heat source problem using fundamental solutions and RBFs*, Engineering Analysis with Boundary Elements, *64* (2016), 278-289.

[7] MD. Buhmann, *Radial basis functions: theory and implementations. Cambridge monographs on applied and computational mathematics,* vol. 12. Cambridge: Cambridge University Press; 2003.

[8] V. Bayona, M. Moscoso, M. Carretero, and M. Kindelan, *RBF-FD formulas and convergence properties,* J. Comput. Phys, *229*(22) (2010), 8281-8295.

[9] V. Bayona, M. Moscoso, and M. Kindelan, *Gaussian RBF-FD weights and its corresponding local truncation errors,* Eng. Anal. Bound. Elem, *36*(9) (2012), 1361-1369.

[10] V. Bayona, M. Moscoso, and M. Kindelan, *Optimal constant shape parameter for multiquadric based RBF-FD method,* J. Comput. Phys, *230*(19) (2011), 7384-7399.

[11] V. Bayona, M. Moscoso, and M. Kindelan, *Optimal variable shape parameter for multiquadric based RBF-FD method,* J. Comput. Phys, *231*(6) (2012), 2466-2481.

[12] J. Brajard, P. Li, F. Jezequel, H. S. Benavidès, and S. Thiria, *Numerical Validation of Data Assimilation Codes Generated by the YAO Software.* In SIAM Annual Meeting, San Diego, California (USA), July 2013.

[13] J. M. Chesneaux and F. Jezequel, *Dynamical Control of Computations Using the Trapezodial and Simpson's rules*, J. Universal Comput. Sc, *4* (1998), 2-10.

[14] J. M. Chesneaux, *Modelisation et conditions de validite de la methode CESTAC*, C. R. Acad. Sci. Paris Sér. I Math, *307* (1988), 417-422.

[15] J .M. Chesneaux and J. Vignes, *Les fondements de larithmetique stochastique*, C. R. Acad. Sci. Paris Sér. I Math, *315* (1992), 1435-1440.
[16] J. M. Chesneaux, *CADNA: An ADA tool for round-off errors analysis and for numerical debugging,* In ADA in Aerospace, Barcelone, Spain, December 1990.
[17] M. A. Fariborzi Araghi, *The methods of valid implementation of the numerical algorithms*, Phd dissertation thesis, Science and research branch, Islamic Azad university, 2002.
[18] M. A. Fariborzi Araghi, and H. Barzegar Kelishami, *Dynamical control of accuracy in the fuzzy Runge-Kutta methods to estimate the solution of a fuzzy differential equation*, Journal of Fuzzy Set Valued Analysis 2016 SI, *1* (2016), 71-84.
[19] E. Isaacson and H. B. Keller, *Analysis of Numerical Methods*, Wiley, New York, 1966.
[20] F. Jezequel, *Controle dynamique de methodes dapproximation, Habilitation a diriger des recherches*, Universit e Pierre et Marie Curie, Paris, 2005.
[21] F. Jezequel, J. L. Lamotte, and O. Chubach, *Parallelization of Discrete Stochastic Arithmetic on multicore architectures.* In 10th International Conference on Information Technology: New Generations (ITNG), Las Vegas, Nevada (USA), 2013.
[22] F. Jezequel, J. L. Lamotte, and I. Said, *Estimation of numerical reproducibility on CPU and GPU.* In 8th Workshop on Computer Aspects of Numerical Algorithms (CANA), Federated Conference on Computer Science and Information Systems (FedCSIS), (2015), 687-692.
[23] F. Jezequel and J. M. Chesneaux, *CADNA: a library for estimating round-off error propagation*, Computer Physics Communications, *178*(12) (2008), 933-955.
[24] F. Jezequel, F. Rico, J. M. Chesneaux, and M. Charikhi, *Reliable computation of a multiple integral involved in the neutron star theory*, Mathematics and Computers in Simulation, *71*(1) (2006), 44-61.
[25] E. J. Kansa and P. Holoborodko, *On the ill-conditioned nature of C^∞ RBF strong collocation*, Anal. Bound. Elem, *78* (2017), 26-30.
[26] E. J. Kansa, *Multiquadrics-a scattered data approximation scheme with applications to computational fluid dynamics II: solutions to parabolic, hyperbolic, and elliptic partial differential equations*, Comput. Math. Appl, *19*(8/9) (1990) 147-161.
[27] D. Khojasteh Salkuyeh, F. Toutounian, and H. Shariat Yazdi, *A procedure with stepsize control for solving n one-dimensional IVPs*, Math. Comput in Simulation, *79*(2) (2008) 167-176.
[28] L. T. Luh, *The mystery of the shape parameter IV*, Eng Anal Boundary Elem, *48* (2014), 24-31.
[29] L. T. Luh, *The shape parameter in the Gaussian function II*, Eng Anal Boundary Elem, *37* (2013), 988-93.
[30] S. A. Sarra and D. Sturgill, *A random variable shape parameter strategy for radial basis function approximation methods*, Eng. Anal. Bound. Elem, *33*(11) (2009), 1239-1245.
[31] S. A. Sarra, *Radial basis function approximation methods with extended precision floating point arithmetic*, Eng. Anal. Bound. Elem, *35*(1) (2011), 68-76.
[32] S. A. Sarra, *Adaptive radial basis function methods for time dependent partial differential equations*, Appl Numer Math, *54*(1) (2005), 79-94.
[33] R. Schaback, *Error estimates and condition numbers for radial basis function interpolation*, AICM, *3* (1995), 251-264.
[34] IJ. Schoenberg, *Metric spaces and completely monotone functions*, Ann Math, *39* (1938), 811-41.
[35] N. S. Scott, F. Jézéquel, C. Denis, and J. M. Chesneaux, *Numerical 'health check' for scientific codes: the CADNA approach*, Computer Physics Communications, *176*(8) (2007), 507-521.
[36] Kh. Tabatabaei and E. Gunerhan, *Numerical Solution of Duffing Equation by the Differential Transform Method*, Appl. Math. Inf. Sci. Lett, *2*(1) (2014), 1-6.
[37] S. Xiang, K. Wang, Y. Ai, Y. Sha, and H. Shi, *Trigonometric variable shape parameter and exponent strategy for generalized multiquadric radial basis function approximation*, Appl. Math. Model, *36*(5) (2012), 1931-1938.
[38] E. Yusufoglu, *Numerical solution of Duffing equation by the Laplace decomposition algorithm*, App. Math. and Comp, *177*(2) (2006), 572-580.
[39] M. Uddin, *On the selection of a good value of shape parameter in solving time-dependent partial differential equations using RBF approximation method*, Appl Math Model, *38*(1) (2014) 135-144.

[40] H. Wendland, *Piecewise polynomial, positive definite and compactly supported radial functions of minimal degree.* Adv Comput Math, *4* (1995), 389-96.
[41] J. Vignes, *A stochastic arithmetic for reliable scientific computation*, Math. Comp. Simul, *35*(3) (1993), 233-261.
[42] J. Vignes. *Zero mathematique et zero informatique*, Comptes Rendus de Academie des Sciences Series I - Mathematics, 303:997–1000, 1986. also: La Vie des Sciences, *4* (1987), 1-13.
[43] J. Vignes, *Discrete stochastic arithmetic for validating results of numerical software,* Numerical Algorithms, 37 (2004), 377-390.
[44] J. Vignes, M. La Porte, *Error analysis in computing*,Information Processing, North-Holland, (1974), 610-614.
[45] J. Vignes, *A stochastic approach to the analysis of round-off error propagation. A survey of the CESTAC method*, Proc. 2nd Real Numbers and Computers Conference, Marseille, France, (1996), 233-251.
[46] Z. Wu, R. Schaback, *Local error estimates for radial basis function interpolation of scattered data*, IMA journal of Numerical Analysis, *13* (1), 13-27.